Title
Generation of knock-in primary human T cells using Cas9 ribonucleoproteins.

Journal
Proceedings of the National Academy of Sciences of the United States of America, 112(33)

ISSN
0027-8424

Authors
Schumann, Kathrin
Lin, Steven
Boyer, Eric
et al.

Publication Date
2015-08-01

DOI
10.1073/pnas.1512503112

Peer reviewed

Generation of knock-in primary human T cells using Cas9 ribonucleoproteins

Kathrin Schumann[a,b,1], Steven Lin[c,1], Eric Boyer[a,b], Dimitre R. Simeonov[a,b,d], Meena Subramaniam[e,f], Rachel E. Gate[e,f], Genevieve E. Haliburton[a,b], Chun J. Ye[e], Jeffrey A. Bluestone[a], Jennifer A. Doudna[c,g,h,i,j,2], and Alexander Marson[a,b,g,2]

[a]Diabetes Center, University of California, San Francisco, CA 94143; [b]Division of Infectious Diseases, Department of Medicine, University of California, San Francisco, CA 94143; [c]Department of Molecular and Cell Biology, University of California, Berkeley, CA 94720; [d]Biomedical Sciences Graduate Program, University of California, San Francisco, CA 94143; [e]Department of Epidemiology and Biostatistics, Department of Bioengineering and Therapeutic Sciences, Institute for Human Genetics, University of California, San Francisco, CA 94143; [f]Biological and Medical Informatics Graduate Program, University of California, San Francisco, CA 94158; [g]Innovative Genomics Initiative, University of California, Berkeley, CA 94720; [h]Howard Hughes Medical Institute, University of California, Berkeley, CA 94720; [i]Department of Chemistry, University of California, Berkeley, CA 94720; and [j]Physical Biosciences Division, Lawrence Berkeley National Laboratory, Berkeley, CA 94720

Contributed by Jennifer A. Doudna, June 29, 2015 (sent for review January 23, 2015)

T-cell genome engineering holds great promise for cell-based therapies for cancer, HIV, primary immune deficiencies, and autoimmune diseases, but genetic manipulation of human T cells has been challenging. Improved tools are needed to efficiently "knock out" genes and "knock in" targeted genome modifications to modulate T-cell function and correct disease-associated mutations. CRISPR/Cas9 technology is facilitating genome engineering in many cell types, but in human T cells its efficiency has been limited and it has not yet proven useful for targeted nucleotide replacements. Here we report efficient genome engineering in human CD4$^+$ T cells using Cas9:single-guide RNA ribonucleoproteins (Cas9 RNPs). Cas9 RNPs allowed ablation of CXCR4, a coreceptor for HIV entry. Cas9 RNP electroporation caused up to ∼40% of cells to lose high-level cell-surface expression of CXCR4, and edited cells could be enriched by sorting based on low CXCR4 expression. Importantly, Cas9 RNPs paired with homology-directed repair template oligonucleotides generated a high frequency of targeted genome modifications in primary T cells. Targeted nucleotide replacement was achieved in *CXCR4* and *PD-1* (*PDCD1*), a regulator of T-cell exhaustion that is a validated target for tumor immunotherapy. Deep sequencing of a target site confirmed that Cas9 RNPs generated knock-in genome modifications with up to ∼20% efficiency, which accounted for up to approximately one-third of total editing events. These results establish Cas9 RNP technology for diverse experimental and therapeutic genome engineering applications in primary human T cells.

CRISPR/Cas9 | genome engineering | Cas9 ribonucleoprotein | RNP | primary human T cells

The CRISPR/Cas9 system has been used increasingly to edit mammalian germline sequence and cell lines (1, 2). Considerable efforts are underway to use this powerful system directly in primary human tissues, but efficiency has been limited, especially in human CD4$^+$ T cells. Plasmid delivery of *cas9* and single-guide RNAs (sgRNAs) was efficient in other cell types, but ablated only 1–5% of target protein expression in CD4$^+$ T cells (3). Improved ability to ablate key targets and correct pathogenic genome sequence in human T cells would have direct therapeutic applications, eventually allowing T cells to be edited ex vivo and then reintroduced into patients.

Multiple scientific and clinical trials are underway to manipulate T-cell genomes with available technologies, including gene deletions with transcription activator-like effector nucleases and zinc finger nucleases and exogenous gene introduction by viral transduction (4, 5). Genetic manipulations have been attempted to "knock out" HIV coreceptors CXCR4 and CCR5 in T cells to gain resistance to HIV infection (6–8). There also has been marked success in engineering T cells to recognize and kill hematological malignancies, but additional genetic modifications appear necessary for solid organ tumor immunotherapy (9–11). Deletion of genes that encode key immune checkpoints such as PD-1 could prove useful for these efforts (12, 13). Further therapeutic opportunities would be possible if targeted T-cell genomic loci could be corrected with specific replacement sequence, rather than deleted (14). Efficient technology to promote homologous recombination in T cells could eventually allow therapeutic correction of mutations that affect specialized T-cell functions.

Recent reports in mammalian cell lines demonstrate that Cas9 ribonucleoproteins (RNPs; recombinant Cas9 protein complexed with an in vitro-transcribed single-guide RNA) can accomplish efficient and specific genome editing (15–17). Here we show that electroporation of Cas9 RNPs leads to efficient genome editing of CD4$^+$ T cells. We were able to ablate a target gene with the random insertion and deletion mutations that likely result from nonhomologous end joining (NHEJ) repair of a Cas9-induced double-stranded DNA break (DSB). Cells with genomic edits in *CXCR4* could be enriched by sorting based on low CXCR4 expression. We were also able to introduce precisely targeted nucleotide replacements in primary T cells at *CXCR4* and *PD-1* by homology-directed repair (HDR) using Cas9 RNPs and exogenous single-stranded DNA templates. This technology enabled Cas9-mediated generation of "knock-in" primary human T cells. Deep sequencing of a target site confirmed that Cas9 RNPs promoted knock-in

Significance

T-cell genome engineering holds great promise for cancer immunotherapies and cell-based therapies for HIV, primary immune deficiencies, and autoimmune diseases, but genetic manipulation of human T cells has been inefficient. We now have achieved efficient genome editing by delivering Cas9 protein pre-assembled with guide RNAs. These active Cas9 ribonucleoproteins (RNPs) enabled successful Cas9-mediated homology-directed repair in primary human T cells. Cas9 RNPs provide a programmable tool to replace specific nucleotide sequences in the genome of mature immune cells—a longstanding goal in the field. These studies establish Cas9 RNP technology for diverse experimental and therapeutic genome engineering applications in primary human T cells.

Author contributions: K.S., S.L., J.A.D., and A.M. designed research; K.S., S.L., E.B., and D.R.S. performed research; K.S., S.L., E.B., D.R.S., M.S., R.E.G., G.E.H., C.J.Y., J.A.B., J.A.D., and A.M. analyzed data; and K.S., S.L., and A.M. wrote the paper.

Conflict of interest statement: J.A.D. is a co-founder of Caribou Biosciences Inc. and Editas Medicine and is on the scientific advisory board of Caribou Biosciences Inc. The A. M. laboratory receives sponsored research support from Epinomics. A patent has been filed based on the findings described here.

Freely available online through the PNAS open access option.

Data deposition: The sequence reported in this paper has been deposited in the ▪▪▪▪▪▪ database (accession no. ▪▪▪).

[1]K.S. and S.L. contributed equally to this work.

[2]To whom correspondence may be addressed. Email: alexander.marson@ucsf.edu or doudna@berkeley.edu.

This article contains supporting information online at www.pnas.org/lookup/suppl/doi:10.1073/pnas.1512503112/-/DCSupplemental.

genome modifications with up to ~20% efficiency (~22% was achieved with 50 pmol and ~18% with 100 pmol of HDR template), which accounted for up to approximately one-third of the total editing events. These findings suggest that Cas9 RNP-mediated nucleotide replacement could eventually prove useful for therapeutic correction of disease-associated mutations. Our study establishes Cas9 RNP technology for experimental and therapeutic knock-out and knock-in editing of the genome in primary human T cells.

Results

We aimed to overcome long-standing challenges in genetic manipulation of primary T cells and establish an efficient genome engineering toolkit. Recent reports in mammalian cell lines suggest that Cas9 RNPs can accomplish efficient and specific genome editing (15–18). Given the significant challenges of efficient genome editing of T cells with DNA delivery of Cas9, we tested the efficacy of Cas9 RNP delivery for targeted genome editing in primary human T cells (Fig. 1*A*).

Ablation of HIV Coreceptor CXCR4 with Cas9 RNPs. A major goal in T-cell engineering is targeted ablation of specific cell-surface receptors, including coreceptors for HIV infection and coinhibitory immune checkpoints that impair tumor immune response. Here, we programmed the Cas9 RNPs to target the exonic sequence of *CXCR4*, which encodes a chemokine receptor with multiple roles in hematopoiesis and cell homing that is expressed on $CD4^+$ T cells and serves as a coreceptor for HIV entry (19–21). We purified recombinant *Streptococcus pyogenes* Cas9 carrying two nuclear localization signal sequences fused at the C terminus. This Cas9 protein was incubated with in vitro-transcribed sgRNA designed to uniquely recognize the human *CXCR4* genomic sequence (Fig. 1*B*). These preassembled Cas9 RNP complexes were electroporated into human $CD4^+$ T cells isolated from healthy donors.

Electroporation of *CXCR4* Cas9 RNPs caused efficient, site-specific editing of genomic DNA. The Cas9 RNP-induced DSBs in the *CXCR4* gene were likely repaired by NHEJ, a predominant DNA repair pathway in cells that gives rise to variable insertions and deletions (indels) and often results in frameshift mutations and loss of gene function (22). Flow cytometry revealed a Cas9 RNP dose-dependent increase in the percentage of T cells expressing low levels of CXCR4, consistent with mutation of the *CXCR4* gene (Fig. 1*C*). The T7 endonuclease 1 (T7E1) assay is a convenient method to assess editing at specific sites in the genome. Here, T7E1 assay confirmed genomic DNA editing at the CXCR4 locus in cells treated with CXCR4 Cas9 RNPs, but not in control cells treated with Cas9 protein alone (no sgRNA; CTRL). Cas9 RNP-treated cells were separated based on CXCR4 expression with fluorescence-activated cell sorting (FACS). Using the T7E1 assay, we found an enrichment of editing in the $CXCR4^{lo}$ cells (15–17%) compared with $CXCR4^{hi}$ cells (4–12% with varying doses of Cas9 RNP) (Fig. 1*D*). Sanger sequencing of the target *CXCR4* genomic site, performed to directly identify editing events, suggested that the T7E1 assay may have underestimated editing efficiency. The T7E1 assay uses denaturation and hybridization of the wild-type and mutant sequences to create a mismatch DNA duplex, which is then digested by T7 endonuclease. However, hybridization of the mismatch duplex may be inefficient, especially when the indel mutation is drastically different from the wild-type sequence, making self-hybridization an energetically more favorable product. Other potential reasons for observed underestimation of editing efficiency with endonuclease assays include incomplete duplex melting, inefficient cleavage of single-base-pair indels, and deviation from the expected 300- and 600-bp products on the agarose gel as a result of large genome edits (23). Sequencing of the *CXCR4* gene in $CXCR4^{lo}$ cells showed that 5/6 clones had mutations/deletions whereas such mutations/deletions were observed in only 4/10 clones and 0/9 clones in $CXCR4^{hi}$ and CTRL-treated $CXCR4^{lo}$ cells, respectively. Importantly, none of the observed edits in the $CXCR4^{hi}$ population terminated the coding sequence (one missense mutation and three in-frame deletions), consistent with the maintenance of protein expression. By contrast, the $CXCR4^{lo}$ population was enriched for cells with a more extensive mutational burden in the

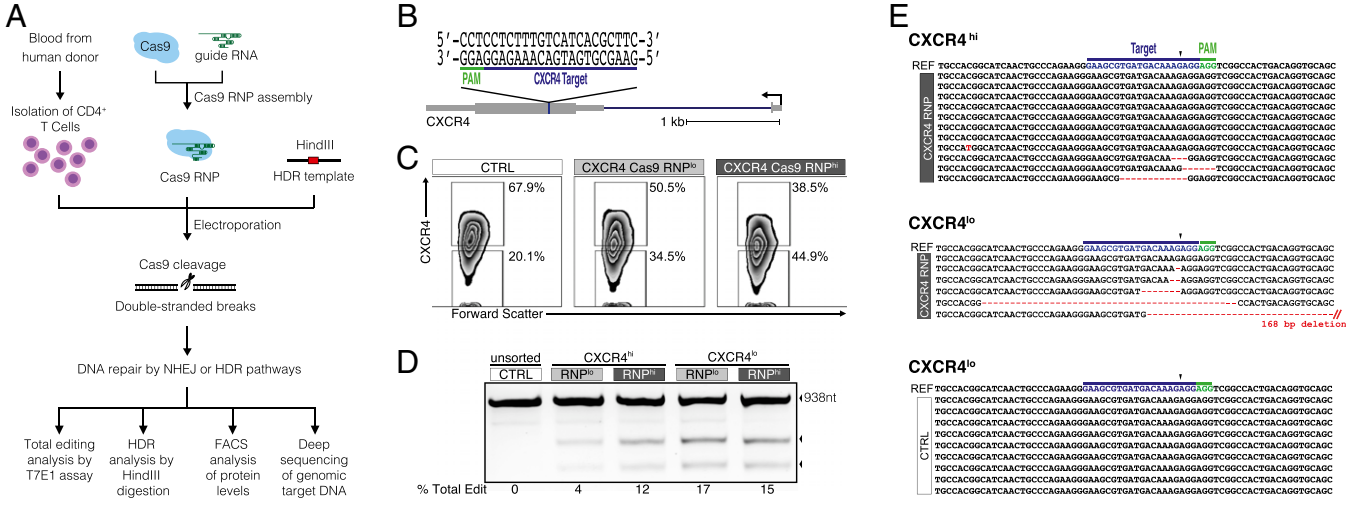

Fig. 1. Efficient editing of *CXCR4* in primary human $CD4^+$ T cells. (*A*) Experimental scheme of Cas9:single-guide RNA ribonucleoprotein (Cas9 RNP) delivery to primary human $CD4^+$ T cells for genome editing, followed by genetic and phenotypic characterization. (*B*) Schematic representation of sgRNA target (blue) and PAM (green) sequence designed to edit coding sequence in the human *CXCR4* locus. (*C*) FACS plots show increasing percentages of cells with low CXCR4 expression ($CXCR4^{lo}$) with higher concentrations of CXCR4 Cas9 RNP (Cas9 RNP ^{lo}: 0.9 μM; Cas9 RNP ^{hi}: 1.8 μM) compared with control-treated cells (Cas9 without sgRNA, CTRL; final concentration: 1.8 μM). (*D*) T7 endonuclease I (T7E1) assay demonstrates genome editing in the *CXCR4* locus with more editing observed in FACS-sorted $CXCR4^{lo}$ cells than in $CXCR4^{hi}$ cells. Expected PCR product size (938 nt) and approximate expected sizes of T7E1-digested fragments are indicated. The total editing frequencies are indicated as percentage of Total Edit below the agarose gel image. (*E*) Mutation patterns detected by cloning and Sanger sequencing of the *CXCR4* locus in sorted Cas9 RNP (1.8 μM)-treated $CXCR4^{hi}$ and $CXCR4^{lo}$ cells are compared with the sequence from $CXCR4^{lo}$ control-treated cells (CTRL). Reference (REF) sequence is shown on top of clonal sequences from each population with sgRNA target (blue) and PAM (green) sequences indicated. Red dashes denote deleted bases, and red sequences indicate mutated nucleotides. Arrowhead indicates the predicted Cas9 cut site. Poor quality sequences obtained from three additional $CXCR4^{lo}$ clones were removed from the sequence alignment.

locus (Fig. 1*E*). These findings demonstrated successful genomic targeting with Cas9 RNPs and a functional effect on protein expression in human CD4$^+$ T cells. Importantly, FACS was able to enrich the population of edited cells, providing an additional useful tool for Cas9 RNP applications in primary T cells.

Efficient Genetic Knock-In with Homology-Directed Repair. Exogenous template-mediated HDR is a powerful technique for precise gene modifications that would enable experimental and therapeutic editing of specific variant sequences. Given the high editing efficiency of Cas9 RNPs, we next tested whether we could achieve exogenous template-mediated HDR in primary T cells. We used a single-stranded oligonucleotide DNA template (HDR template) with 90 nucleotide homology arms to recombine with the *CXCR4* locus at the Cas9 RNP cleavage site (16). The CXCR4 HDR template was designed to replace 12 nucleotides from the human reference genome, including the protospacer adjacent motif (PAM) sequence required for CRISPR-mediated DNA cleavage, and to introduce a HindIII restriction enzyme cleavage site (Fig. 2*A*). Cas9 RNPs were electroporated into primary CD4$^+$ T cells in the presence of four different concentrations of CXCR4 HDR template (0, 50, 100, and 200 pmol; *SI Materials and Methods*). Cas9 RNP without HDR template again reduced the percentage of CXCR4^{hi} cells. Notably, in this experiment, addition of the CXCR4 HDR template significantly improved the efficacy of CXCR4 ablation, although this effect on cell-surface expression was not seen in all experiments (Fig. S1*A*). In the experiment shown here, ~60% of cells lost high-level cell-surface CXCR4 expression with 100 pmol HDR template and Cas9 RNP (1 vs. 60% in control-treated cells) (Fig. 2 *B* and *C*).

Remarkably efficient HDR was observed in cells treated with Cas9 RNP and the single-stranded oligonucleotide HDR template (Fig. 2*D*). Up to 33% total editing (defined as the sum of all NHEJ and HDR events that give rise to indels at Cas9 cleavage site) was observed in the presence of 50 pmol CXCR4 HDR template, as estimated by T7E1 assays. At this concentration, 14% HDR was estimated by HindIII digest of the target locus, indicating that a high fraction of editing resulted from HDR (see results below for further quantification). The nearly complete loss of CXCR4 staining with addition of the HDR template suggests that the mutation introduced by HDR (84DLLFV88 → 84ESLDP88) strongly affected the cell-surface expression of CXCR4 or its recognition by the antibody (Fig. 2 *B* and *C*). The editing efficiency was reduced with 200 pmol HDR template, perhaps as a result of cellular toxicity.

Both total editing and HDR could be enriched by sorting the CXCR4^{lo} population, although the effect was less pronounced than in Fig. 1, consistent with the larger fraction of CXCR4^{lo} cells in the unsorted population. Note that in these experiments a more stringent gate was applied to separate the cells with the highest expression of CXCR4, and in this CXCR4^{hi} population no editing was observed. These studies collectively demonstrated the power of Cas9 RNPs coupled with single-stranded oligonucleotide HDR template to precisely replace targeted DNA sequences in primary human T cells.

Deep Sequencing of Target Genomic DNA. Deep sequencing of the targeted *CXCR4* locus allowed more detailed and quantitative analysis of genome-editing events. The results highlighted in Fig. 3 show the frequency of insertions, deletions, and HDR-mediated nucleotide replacement in CXCR4 Cas9 RNP-treated cells with or without CXCR4 HDR template compared with control-treated cells. In CXCR4 Cas9 RNP-treated cells, we found 55% of reads overlapping the *CXCR4* target site containing at least one indel within a 200-nucleotide window centered around the expected cut site (Fig. 3 *A* and *B* and Dataset S1). As discussed above, the T7E1 assays are useful for identifying edited loci, but may underestimate actual editing efficiency (quantitation of the T7E1 assay in Fig. 2*D* suggested 33% editing

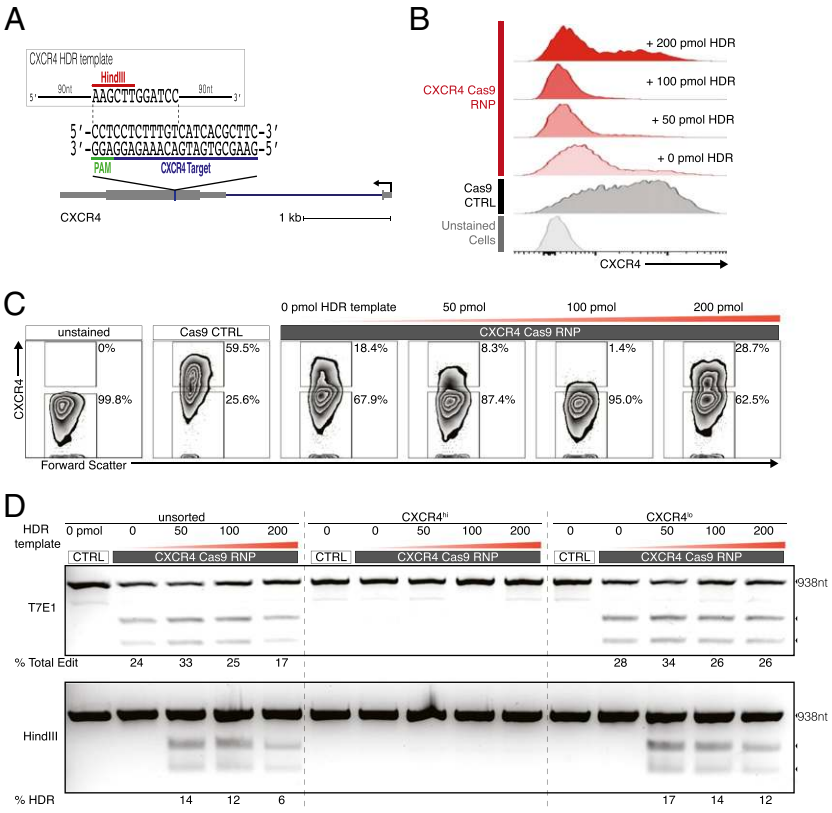

Fig. 2. Efficient homology-directed repair allows targeted DNA replacement in primary human T cells. (*A*) Schematic representation of single-stranded oligonucleotide HDR template with 90-nt homology arms designed to replace 12 nt, including the PAM sequence, and introduce a novel HindIII restriction enzyme cleavage site (red) at the *CXCR4* locus, where the Cas9 RNP cleaves. sgRNA target (blue) and PAM (green) sequence are indicated. (*B*) Histograms of CXCR4 cell-surface staining assessed by flow cytometry in CXCR4 Cas9 RNP-treated cells in the presence of varying concentrations of single-stranded HDR template (compared with control Cas9 protein-treated cells and unstained cells). (*C*) FACS plots (corresponding to histograms in *B*) show maximal ablation of CXCR4 with Cas9 RNP treatment and 100 pmol of HDR template. (*D*) T7E1 assay was used to estimate the "% Total Edit" (defined as the sum of all NHEJ and HDR events that gives rise to indels at the Cas9 cleavage site), whereas HDR frequency was determined by HindIII digestion, which specifically cleaved the newly integrated HindIII site, and was calculated as the ratio of DNA product to DNA substrate. Expected PCR product size (938 nt) and approximate expected T7E1 and HindIII digestion fragments are indicated.

compared with the 55% editing efficiency computed by deep sequencing). We also sequenced the two top predicted "off-target" sites for the CXCR4 Cas9 RNP (Fig. 3*B*). Rare indels were observed at both off-target sites (~1–2%), but at a rate comparable to that observed for those sites in the control cells treated with Cas9 protein only (~1–2%) (Dataset S1).

The deep-sequencing results allowed quantitative analysis of observed indel mutations and their spatial distribution in the target region. Consistent with reports that *S. pyogenes* Cas9 cuts about three nucleotides upstream from the PAM sequence, we found the highest frequency of indels at four nucleotides upstream of the PAM (Fig. 3*A*). Indels were distributed throughout the sequenced region (Fig. 3 *C* and *D*) with the majority of events near cut sites (>94% within 40 nucleotides). In CXCR4 Cas9 RNP-treated cells within ±100 nucleotides from the cut site, we observed that 95% of reads with indels contained a deletion event whereas 10% contained an insertion event (Dataset S1). Interestingly, of the reads with insertion events, ~50% also contained at least one deletion. We observed a wide range of insertion and deletion sizes, with many reads exhibiting deletions up to ~80 nucleotides in length (mean: 18 nucleotides; SD: 15 nucleotides) and some insertions up to ~55 nucleotides in length (mean: 4.4 nucleotides; SD: 4.8 nucleotides) (Fig. 3 *C* and *D* and Fig. S2). This range of indel sizes and locations was consistent with the extensive mutational burden observed in Sanger sequencing of CXCR4^{lo} selected cells in Fig. 1.

Deep sequencing verified the successful targeted replacement of 12 nt at the *CXCR4* locus, but only in cells treated with both Cas9 RNPs and CXCR4 HDR template. We observed 25% incorporation of HDR template sequence with 50 pmol HDR template and 21% with 100 pmol HDR template (Fig. 3*A*). Of the reads with HDR template sequence incorporated, ~14% of the detected HDR template reads had additional nonspecific indels surrounding the incorporated HindIII site or other imperfect forms of editing within the 200-nucleotide window centered at the predicted cut site. However, the frequency of indels in reads with the HindIII site incorporated was reduced compared with reads where the HindIII site was not detected (Fig. 3 *C* and *D* and Fig. S2). Interestingly, there was a consistent pattern of deletion events between CXCR4 Cas9 RNP with and without CXCR4 HDR template with an enrichment of deletions of 2 nucleotides (11%) and 22 nucleotides (5.4%) (Fig. S2). Replacement of the PAM sequence likely helped to limit recutting of knock-in sequence. Overall, 18–22% of reads (with varying concentrations of HDR template) had correctly replaced nucleotides throughout the sequenced genomic target site, suggesting that this approach could prove useful for generation of experimental and therapeutic nucleotide knock-in primary human T cells.

Specific Knock-In Targeting of Key Cell-Surface Receptors. To confirm that Cas9 RNPs mediate HDR at other genomic sites, we designed a guide RNA and HDR template to target the *PD-1* (*PDCD1*) locus. PD-1 is an "immune checkpoint" cell-surface receptor found on the surface of chronically activated or exhausted T cells that can inhibit effective T-cell–mediated clearance of cancers. Monoclonal antibody blockade of PD-1 is approved for treatment of advanced malignancy, and genetic deletion of *PD-1* may prove useful in engineering T cells for cell-based cancer immunotherapies (12). Primary human T cells were electroporated with a PD-1 Cas9 RNP and a PD-1 HDR template designed to generate a frameshift mutation and a knock-in a HindIII restriction site in the first exon of *PD-1*, thereby replacing the PAM sequence (Fig. 4*A*).

To examine the specificity of Cas9 RNP-mediated targeting, we compared PD-1 cell-surface expression following treatment with PD-1 Cas9 RNP vs. CXCR4 Cas9 RNP (which should not target

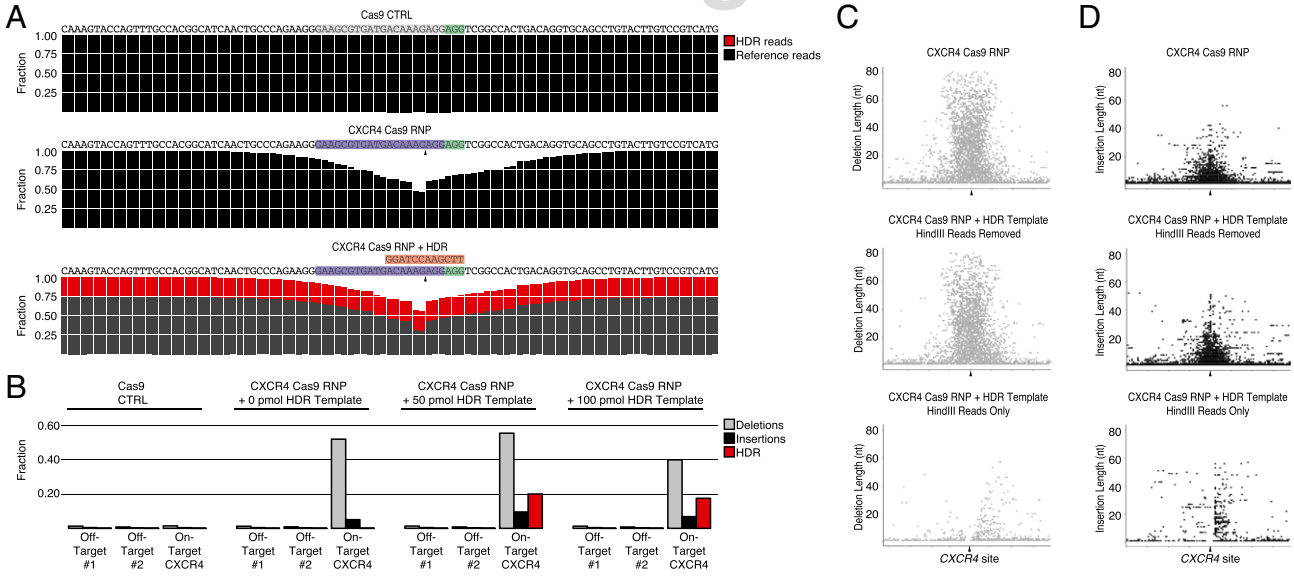

Fig. 3. Quantitative analysis of Cas9 RNP-mediated editing and HDR by deep sequencing. (*A*) CXCR4 Cas9 RNP-mediated indels and HDR from experiments in Fig. 2 were analyzed by targeted deep sequencing of the *CXCR4* locus. A total of 100 nt centered on the predicted cut site are shown with sgRNA target (blue) aand PAM (green), and predicted sequence after HDR genome targeting (red) is indicated. At each position, the fraction of reads that correctly aligned to the reference genome (black) or HDR template-derived sequence (red) are shown. Although rare (~1–2%), edits were detected with Cas9-only control treatment, including at the predicted *CXCR4* cut site, potentially indicating trace amounts of experimental contamination of the Cas9 RNPs. (*B*) Bar graph summarizes the fractions of reads edited with deletions (gray), insertions (black), or successful HDR targeting (red) in Cas9 CTRL, CXCR4 Cas9 RNP, and CXCR4 Cas9 RNP cells with 50 or 100 pmol CXCR4 HDR template at the *CXCR4* site and two predicted off-target sites. Reads with HDR template-derived sequence incorporated were removed to calculate fractions with deletions and insertions (Dataset S1). Scatter plots show the genomic localization (±100 nt around the expected Cas9 cut side; chromosome 2: 136873140–136873340) and the length of (*C*) deletions and (*D*) insertions. (*Top*) Deletions/insertions for CXCR4 RNP-treated cells. (*Middle*) Deletions/insertions in reads without HDR template sequence incorporated in cells treated with CXCR4 RNP and CXCR4 HDR template. (*Bottom*) Deletions/insertions in reads with HDR template-derived sequence incorporated. Arrowheads indicate approximate location of expected Cas9 cut site.

the *PD-1* locus) or scrambled guide Cas9 RNP (no predicted cut within the human genome). We performed replicate experiments side by side with two different blood donors and with sgRNAs generated with two different in vitro transcription protocols (*SI Materials and Methods*). PD-1 Cas9 RNPs electroporated with PD-1 HDR template significantly reduced the percentage of cells with high PD-1 cell-surface expression relative to both CXCR4 Cas9 RNPs and scrambled guide Cas9 RNPs delivered with PD-1 HDR template (Fig. 4*B*). Similarly, CXCR4 Cas9 RNPs and CXCR4 HDR template caused a decrease in the CXCR4^{hi} cell population relative to both PD-1 and scrambled guide Cas9 RNP treatments with CXCR4 HDR template (Fig. 4*C*). Loss of CXCR4 was not a nonspecific effect of single-stranded DNA delivered along with CXCR4 Cas9 RNP; we observed a higher percentage of CXCR4-expressing cells after treatment with CXCR4 Cas9 RNP and scrambled HDR template than with CXCR4 Cas9 RNP and CXCR4 HDR template (Fig. S1*A*). These findings confirmed the target-specific modulation of cell-surface receptor expression in primary T cells with the programmable Cas9 RNP and HDR template treatments.

We then tested the specificity of HDR templates for nucleotide replacement (Fig. 4*D*; examples of corresponding cell-surface expression data are shown in Fig. S1*B*). As expected, we observed efficient *PD-1* editing by PD-1 Cas9 RNPs regardless of whether they were delivered with PD-1 HDR template, CXCR4 HDR template, or without any HDR template. In contrast, the HindIII site was incorporated into *PD-1* only in the presence of both PD-1 Cas9 RNP and PD-1 HDR template, but not with CXCR4 HDR template, which should not be recombined at *PD-1* locus due to the lack of sequence homology. Similarly, a HindIII site was incorporated only into *CXCR4* following treatment with CXCR4 Cas9 RNP and CXCR4 HDR template; HDR was not observed at the *CXCR4* locus with PD-1 HDR template, control scrambled HDR template (with a HindIII site), or without HDR template (Fig. 4*D*). Taken together, these studies established that specific pairing of a programmed Cas9 RNP and corresponding HDR template is required for targeted nucleotide replacement in primary human T cells.

Discussion

Cas9-mediated genome engineering has enormous potential to experimentally and therapeutically target DNA elements crucial for T-cell function. We report here successful genome engineering in human CD4$^+$ T cells by delivery of in vitro-assembled Cas9 RNPs. Electroporation of Cas9 RNPs allowed targeted knock-out of the CXCR4 cell-surface receptor. Cas9 RNPs also promoted successful Cas9-mediated genetic knock-in of specific nucleotides to *CXCR4* and *PD-1* in primary human T cells. The efficient targeted DNA replacement in mature immune cells achieves a longstanding goal in the immunology field to enable diverse research and therapeutic applications. These studies collectively establish a broadly applicable toolkit for genetic manipulation of human primary T cells.

There are notable advantages to genome engineering with transient Cas9 RNP delivery compared with other CRISPR/Cas9 delivery methods. Recent work reported ablation of cell-surface markers in human CD4$^+$ T cells by transfection of plasmid carrying the *cas9* gene and guide RNA-coding sequence (3). Although successful, efficiency was notably low in CD4$^+$ T cells compared with other cell types, possibly due to suboptimal levels of Cas9 or sgRNA, suboptimal nuclear translocation, or suboptimal intracellular Cas9 RNP complex formation (or some combination of these factors). Cas9 RNP-based delivery circumvents these challenges. Delivery of Cas9 RNPs offers fast editing action and rapid protein turnover in the cells as they are reportedly degraded within 24 h of delivery (15). This limited temporal window of Cas9 editing may make Cas9 RNPs safer for therapeutic applications than other

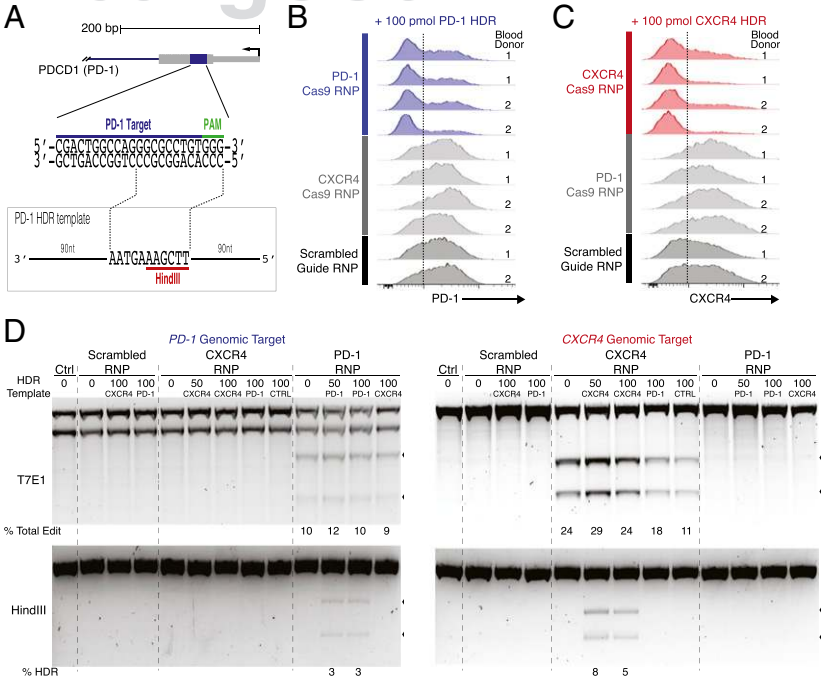

Fig. 4. Cas9 RNPs can be programmed for knock-in editing of PD-1 or CXCR4. (*A*) Schematic representation of the single-stranded PD-1 HDR template with 90-nt homology arms designed to replace 12 nt with 11 nt, introducing a novel HindIII restriction enzyme cleavage site to replace the PAM sequence (red). sgRNA target (blue) and PAM (green) sequences are indicated. (*B*) Histograms of PD-1 cell-surface expression levels assessed by flow cytometry. All cells were treated with 100 pmol of PD-1 HDR template. PD-1 Cas9 RNP-treated cells are shown in blue, CXCR4 Cas9 RNP-treated cells in light gray, and scrambled guide (no predicted cut within the human genome) Cas9 RNP-treated cells in dark gray. (*C*) Histograms of CXCR4 cell-surface expression levels assessed by flow cytometry. All cells were treated with 100 pmol of CXCR4 HDR template. CXCR4 Cas9 RNP-treated cells are shown in red, PD-1 Cas9 RNP-treated cells in light gray, and scrambled guide Cas9 RNP-treated in dark gray. (*B* and *C*) Results of four experiments with two differently in vitro-transcribed and purified CXCR4 and PD-1 sgRNAs (*SI Materials and Methods*) tested in two different blood donors. For each blood donor, experiments done with phenol/chloroform-extracted sgRNAs are shown on *Top* and experiments with PAGE-purified sgRNAs are shown at the *Bottom*; scrambled guides were prepared for both experiments with phenol/chloroform extraction. Dotted line indicates gating on PD-1 high-expressing or CXCR4 high-expressing cells, respectively. The percentage of PD-1 high-expressing cells was significantly lower with PD-1 Cas9 RNP treatment compared either CXCR4 Cas9 RNP treatment ($P < 0.001$) or scrambled guide Cas9 RNP treatment ($P < 0.001$). The percentage of CXCR4 high-expressing cells was significantly lower with CXCR4 Cas9 RNP treatment compared with either PD-1 Cas9 RNP treatment ($P < 0.001$) or scrambled guide Cas9 RNP treatment ($P < 0.001$) (Pearson's χ^2). (*D*) Genome editing was analyzed by T7E1 assay, whereas HDR was detected by HindIII digestion, which specifically cleaved the newly integrated HindIII site; cleavage products for both assays are indicated with arrowheads. Concentrations of various HDR templates are indicated above the agarose gels. CTRL HDR template refers to a scrambled version of the original CXCR4 HDR template, including a HindIII restriction site. A nonspecific second gel band of unclear significance was noted in the T7E1 of the *PD-1* amplicon under all conditions. Total editing and HDR frequencies were calculated and are displayed below agarose gel images.

delivery modes where cells are exposed to Cas9 for a longer time frame. Further testing will be needed to assess the purity of Cas9 RNPs and potential off-target effects before any clinical use. Our findings now suggest that Cas9 RNPs are able to rapidly and efficiently edit human T cells.

We were able to achieve remarkably efficient HDR here with almost complete loss of the CXCR4^{hi} cell population with Cas9 RNPs and an HDR template targeting CXCR4 in one experiment. Up to 25% of the reads showed incorporation of HDR template sequence in the *CXCR4* locus, and ~20% of the reads showed correctly replaced sequence throughout the target site with no additional indels. Future studies will optimize remaining variables that affect editing and HDR efficiency in primary T cells. We recently demonstrated in cultured cell lines that variation in cell type and cell cycle dynamics significantly alter Cas9 RNP efficiency (16). In primary human T cells, editing efficiency could also be affected by T-cell donor-specific factors (e.g., genetics, recent infection), in vitro T-cell activation status, and characteristics of the targeted genomic locus (e.g., DNA sequence, chromatin state). Characterizing these variables and further optimizing genome engineering efficiency will accelerate the experimental and therapeutic editing of T cells using Cas9 RNPs.

The ability to edit specific DNA sequences in human T-cell subsets will enable experimental investigation of transcription factors, *cis*-regulatory elements, and target genes implicated in T-cell inflammatory and suppressive functions. Extensive efforts have mapped key gene regulatory circuitry controlling the development and function of diverse and specialized T-cell subsets (24). We recently reported that most causal genetic variants contributing to risk of human autoimmune diseases map to key regulatory elements in T cells (25). Looking forward, genome editing of primary T cells will now provide a powerful perturbation test to assess the function of regulatory elements and characterize the effects of disease-associated coding and noncoding variation.

Therapeutic editing requires improved techniques to identify successfully edited cells in a population. Selection of edited cells is notably challenging in primary cells that cannot be maintained indefinitely in culture, unlike transformed cell lines. Here we demonstrate FACS enrichment of edited cells based on expected phenotypic changes in cell-surface receptor expression. The success of Cas9 RNP-mediated HDR should also allow introduction of genetic markers to purify homogenously edited cells for further functional characterization and potentially also for therapeutic applications.

Therapeutic T-cell engineering requires efficient and precisely targeted genome editing in primary cells. The Cas9 RNP technology reported here should accelerate efforts to correct genetic variants and engineer human T-cell function for the treatment of infection, autoimmunity, and cancer.

Materials and Methods

Human T-cell Isolation and Culture. Human primary T cells were either isolated from fresh whole blood or buffy coats. Peripheral blood mononuclear cells (PBMCs) were isolated by Ficoll gradient centrifugation. CD4$^+$ T cells were pre-enriched with an Easysep Human CD4$^+$ T-cell enrichment kit (Stemcell Technologies) according to the manufacturer's protocol. Pre-enriched CD4$^+$ T cells were stained with following antibodies: αCD4-PerCp (SK3; Becton Dickinson), αCD25-APC (BC96; TONBO Biosciences), αCD127-PE (R34-34; TONBO Biosciences), αCD45RA-violet-Fluor450 (HI100; TONBO Biosciences), and αCD45RO-FITC (UCHL1; TONBO Biosciences). CD4$^+$CD25^{lo}CD127^{hi} T effectors (Teffs) were isolated using a FACS Aria IIIu (Becton Dickinson).

Cas9 RNP Assembly and Electroporation. Cas9 RNP was prepared immediately before experiments by incubating 20 μM Cas9 with 20 μM sgRNA at 1:1 ratio in 20 μM Hepes (pH 7.5), 150 mM KCl, 1 mM $MgCl_2$, 10% glycerol and 1 mM Tris(2-chloroethyl) phosphate (TCEP) at 37 °C for 10 min to a final concentration of 10 μM. T cells were electroporated with a Neon transfection kit and device (Invitrogen). Q:17

Analysis of Genome Editing. Editing efficiency was estimated by T7 endonuclease I assay. HDR templates were designed to introduce a HindIII restriction site into the targeted gene loci; successful HDR was confirmed with HindIII restriction enzyme digestion. The genomic region flanking the Cas9 target site for the CXCR4 on-target and two off-target genes was amplified by the two-step PCR method. Sequencing libraries were sequenced with the Illumina HiSEq. 2500.

See *SI Materials and Methods* for further details.

ACKNOWLEDGMENTS. We thank Mary Rieck, Jacqueline Howells, Amy Putnam, and Caroline Raffin in the J.A.B. laboratory; Richard Lao and the University of California at San Francisco (UCSF) Institute for Human Genetics Genomics Core; Michael Lee, Vinh Nguyen, and the UCSF Flow Cytometry Core; Amy Lee in the Cate laboratory; all members of the A.M., J.A.B., and J.A.D. laboratories for suggestions and technical assistance; and K. M. Ansel for critical reading of the manuscript. This research was supported by the UCSF Sandler Fellowship (to A.M.); a gift from Jake Aronov (to A.M.); NIH funding for the HARC Center (P50GM082250) (to A.M. and J.A.D.); a National MS Society Collaborative Research Centre Award (to A.M. and J.A.D.); and the Howard Hughes Medical Institute (HHMI) (J.A.D.). S.L. is an HHMI Fellow of the Damon Runyon Cancer Research Foundation [DRG-(2176-13)], and G.E.H. is supported by an NIH training grant to UCSF Diabetes, Endocrinology and Metabolism (T32 DK741834). Q:18

1. Doudna JA, Charpentier E (2014) Genome editing. The new frontier of genome engineering with CRISPR-Cas9. *Science* 346(6213):1258096.
2. Hsu PD, Lander ES, Zhang F (2014) Development and applications of CRISPR-Cas9 for genome engineering. *Cell* 157(6):1262–1278.
3. Mandal PK, et al. (2014) Efficient ablation of genes in human hematopoietic stem and effector cells using CRISPR/Cas9. *Cell Stem Cell* 15(5):643–652.
4. Maus MV, et al. (2014) Adoptive immunotherapy for cancer or viruses. *Annu Rev Immunol* 32:189–225.
5. Passerini L, et al. (2013) CD4$^+$ T cells from IPEX patients convert into functional and stable regulatory T cells by FOXP3 gene transfer. *Sci Transl Med* 5(215):215ra174.
6. Hütter G, et al. (2009) Long-term control of HIV by CCR5 Delta32/Delta32 stem-cell transplantation. *N Engl J Med* 360(7):692–698.
7. Didigu CA, et al. (2014) Simultaneous zinc-finger nuclease editing of the HIV coreceptors ccr5 and cxcr4 protects CD4+ T cells from HIV-1 infection. *Blood* 123(1): 61–69.
8. Tebas P, et al. (2014) Gene editing of CCR5 in autologous CD4 T cells of persons infected with HIV. *N Engl J Med* 370(10):901–910.
9. Restifo NP, Dudley ME, Rosenberg SA (2012) Adoptive immunotherapy for cancer: Harnessing the T cell response. *Nat Rev Immunol* 12(4):269–281.
10. Porter DL, Levine BL, Kalos M, Bagg A, June CH (2011) Chimeric antigen receptor-modified T cells in chronic lymphoid leukemia. *N Engl J Med* 365(8):725–733.
11. Moon EK, et al. (2014) Multifactorial T-cell hypofunction that is reversible can limit the efficacy of chimeric antigen receptor-transduced human T cells in solid tumors. *Clin Cancer Res* 20(16):4262–4273.
12. Topalian SL, Drake CG, Pardoll DM (2015) Immune checkpoint blockade: A common denominator approach to cancer therapy. *Cancer Cell* 27(4):450–461.
13. John LB, et al. (2013) Anti-PD-1 antibody therapy potently enhances the eradication of established tumors by gene-modified T cells. *Clin Cancer Res* 19(20):5636–5646.
14. Genovese P, et al. (2014) Targeted genome editing in human repopulating haematopoietic stem cells. *Nature* 510(7504):235–240.
15. Kim S, Kim D, Cho SW, Kim J, Kim JS (2014) Highly efficient RNA-guided genome editing in human cells via delivery of purified Cas9 ribonucleoproteins. *Genome Res* 24(6):1012–1019.
16. Lin S, Staahl BT, Alla RK, Doudna JA (2014) Enhanced homology-directed human genome engineering by controlled timing of CRISPR/Cas9 delivery. *eLife* 3:e04766.
17. Zuris JA, et al. (2015) Cationic lipid-mediated delivery of proteins enables efficient protein-based genome editing in vitro and in vivo. *Nat Biotechnol* 33(1):73–80.
18. Sung YH, et al. (2014) Highly efficient gene knockout in mice and zebrafish with RNA-guided endonucleases. *Genome Res* 24(1):125–131.
19. Zou YR, Kottmann AH, Kuroda M, Taniuchi I, Littman DR (1998) Function of the chemokine receptor CXCR4 in haematopoiesis and in cerebellar development. *Nature* 393(6685):595–599.
20. Berson JF, et al. (1996) A seven-transmembrane domain receptor involved in fusion and entry of T-cell-tropic human immunodeficiency virus type 1 strains. *J Virol* 70(9): 6288–6295.
21. Feng Y, Broder CC, Kennedy PE, Berger EA (1996) HIV-1 entry cofactor: functional cDNA cloning of a seven-transmembrane, G protein-coupled receptor. *Science* 272(5263): 872–877.
22. Symington LS, Gautier J (2011) Double-strand break end resection and repair pathway choice. *Annu Rev Genet* 45:247–271.
23. Guschin DY, et al. (2010) A rapid and general assay for monitoring endogenous gene modification. *Methods Mol Biol* 649:247–256.
24. Vahedi G, et al. (2013) Helper T-cell identity and evolution of differential transcriptomes and epigenomes. *Immunol Rev* 252(1):24–40.
25. Farh KK, et al. (2015) Genetic and epigenetic fine mapping of causal autoimmune disease variants. *Nature* 518(7539):337–343.

AUTHOR QUERIES

AUTHOR PLEASE ANSWER ALL QUERIES 1

Q: 1_Please contact PNAS_Specialist.djs@sheridan.com if you have questions about the editorial changes, this list of queries, or the figures in your article. Please include your manuscript number in the subject line of all email correspondence; your manuscript number is 201512503.

Q: 2_Please (i) review the author affiliation and footnote symbols carefully, (ii) check the order of the author names, and (iii) check the spelling of all author names, initials, and affiliations. Please check with your coauthors about how they want their names and affiliations to appear. To confirm that the author and affiliation lines are correct, add the comment "OK" next to the author line. This is your final opportunity to correct any errors prior to publication. Misspelled names or missing initials will affect an author's searchability. Once a manuscript publishes online, any corrections (if approved) will require publishing an erratum; there is a processing fee for approved erratum.

Q: 3_Please review and confirm your approval of the short title: Cas9 RNP-mediated knock-in human T cells. If you wish to make further changes, please adhere to the 50-character limit. (NOTE: The short title is used only for the mobile app and the RSS feed.)

Q: 4_Please review the information in the author contribution footnote carefully. Please make sure that the information is correct and that the correct author initials are listed. Note that the order of author initials matches the order of the author line per journal style. You may add contributions to the list in the footnote; however, funding should not be an author's only contribution to the work.

Q: 5_You have chosen the open access option for your paper and have agreed to pay an additional $1350 (or $1000 if your institution has a site license). Please confirm this is correct and note your approval in the margin.

Q: 6_Please verify that all supporting information (SI) citations are correct. Note, however, that the hyperlinks for SI citations will not work until the article is published online. In addition, SI that is not composed in the main SI PDF (appendices, datasets, movies, and "Other Supporting Information Files") have not been changed from your originally submitted file and so are not included in this set of proofs. The proofs for any composed portion of your SI are included in this proof as subsequent pages following the last page of the main text. If you did not receive the proofs for your SI, please contact **PNAS_Specialist.djs@sheridan.com**.

Q: 7_Please check the order of your keywords and approve or reorder them as necessary. Note that PNAS allows up to five keywords; please do not add new keywords unless you wish to replace others.

Q: 8_PNAS article titles should be accessible to a broad scientific audience; specialized abbreviations in article titles should be spelled out except for abbreviations that are defined in the abstract. As such, "Cas9" is nonstandard and will need to be spelled out in the title. If this is not possible, please provide a modifier for this term that identifies what the term is (for example, "protein kinase _____").

Q: 9_Please confirm whether full institutional information (e.g., unit/division/department) has been included in each affiliation. PNAS requires smallest institutional unit(s) to be listed for each author in each affiliation.

AUTHOR QUERIES

AUTHOR PLEASE ANSWER ALL QUERIES 2

Q: 10_PNAS discourages claims of priority. In sentence in Significance Statement “We now have achieved...." if this is a claim of priority, please rephrase or remove it altogether to avoid the claim of priority.

Q: 11_PNAS requires gene and protein abbreviations to be defined. Please provide definitions for any gene and protein abbreviations that appear more than once in your paper (it is not necessary to do so for abbreviations that appear only once in the text). If this is not possible, please provide a modifier for each term that identifies what the term is (for example, “protein kinase _____”).

Q: 12_PNAS italicizes genes and alleles. All genes, alleles, and proteins will appear as indicated in your proofs. Please carefully check use of italics and capital letters throughout the proof and correct as necessary. If, by “■■■ gene,” you mean “the gene that encodes protein ■■■,” then italic type is not necessary. (NOTE: If all instances of a gene/allele should be changed, please make only one correction and indicate that it is a global change.)

Q: 13_Please indicate whether the sequences have been deposited in GenBank or another publicly accessible database before your page proofs are returned. It is PNAS policy that the data be deposited BEFORE the paper can be published.

Q: 14_Please provide accession number(s) and name of database where data for your paper have been deposited or delete data deposition footnote.

Q: 15_Sentence beginning "Deep sequencing verified...." ok as edited?

Q: 16_"In contrast, the HindIII site was incorporated into *PD-1* only in the presence" ok as edited?

Q: 17_Throughout please state basis for concentrations >1% (e.g., vol/vol).

Q: 18_In Acknowledgments, please spell out HARC.

Q: 19_PNAS discourages claims of priority. In sentence in Fig. 2 legend beginning "Schematic representation...." is this truly novel? If not, please either (a) replace the term “novel” with a term such as “previously unidentified” or (b) remove it altogether to avoid the claim of priority.

Q: 20_"restriction enzyme cleavage site (red)" ok as edited to reflect actual color in Fig. 2?

Q: 21_PNAS discourages claims of priority. In sentence in Fig. 4 legend beginning "Schematic representation of..." is this truly novel? If not, please either (a) replace the term “novel” with a term such as “previously unidentified” or (b) remove it altogether to avoid the claim of priority.

Supporting Information

Schumann et al. 10.1073/pnas.1512503112

SI Materials and Methods

Human T-Cell Isolation and Culture. Human primary T cells were isolated from either fresh whole blood or buffy coats (Stanford Blood Center). Whole blood was collected from human donors in sodium heparinized vacutainer tubes (Becton Dickinson) with approval by the UCSF Committee on Human Research and processed within 12 h. PBMCs were isolated by Ficoll gradient centrifugation. Fresh blood was mixed in a 1:1 ratio with Ca^{2+} and Mg^{2+} free HBSS, Buffy coats were diluted in a 1:10 ratio with HBSS. Thirty milliliters of the respective HBSS/blood solution were transferred to 50-mL Falcon tubes and underlaid with 12 mL Ficoll-Paque PLUS (Amersham/GE healthcare). After density gradient centrifugation (1,000 × *g*, 20 min, no brakes) the PBMC layer was carefully removed and the cells were washed twice with Ca^{2+} and Mg^{2+} free HBSS. $CD4^+$ T cells were pre-enriched with a Easysep Human $CD4^+$ T-cell enrichment kit (Stemcell Technologies) according to the manufacturer's protocol. Pre-enriched $CD4^+$ T cells were stained with the following antibodies: αCD4-PerCp (SK3; Becton Dickinson), αCD25-APC (BC96; TONBO Biosciences), αCD127-PE (R34-34; TONBO Biosciences), αCD45RA-violetFluor450 (HI100; TONBO Biosciences), and αCD45RO-FITC (UCHL1; TONBO Biosciences). $CD4^+CD25^{lo}CD127^{hi}$ Teffs were isolated using a FACS Aria Illu (Becton Dickinson). Teff purity was >97%.

For Cas9 RNP transfections, the effector $CD4^+$ T cells isolated from whole blood were preactivated on αCD3 (UCHT1; BD Pharmingen) and αCD28 (CD28.2; BD Pharmingen) coated plates for 48 h. Plates were coated with 10 μg/mL αCD3 and αCD28 in PBS for at least 2 h at 37 °C. Buffy coat-derived T cells were activated on plates coated with 10 μg/mL αCD3 (in PBS for at least 2 h at 37 °C) with 5 μg/mL αCD28 added directly to the RPMI complete medium.

The T cells were activated in RPMI complete, RPMI-1640 [UCSF Cell Culture Facility (CCF)] supplemented with 5 mmol/L 4-(2-hydroxyethyl)-1-piperazineethanesulfonic acid (Hepes) (UCSF CCF), 2 mmol/L Glutamax (Gibco), 50 μg/mL penicillin/streptomycin (Corning), 50 μmol/L 2-mercaptoethanol (Sigma-Aldrich), 5 mmol/L nonessential amino acids (Corning), 5 mmol/L sodium pyruvate (UCSF CCF), and 10% FBS (Atlanta Biologicals). After electroporation the medium was supplemented with 40 IU/mL IL-2.

Expression and Purification of Cas9. The recombinant *S. pyogenes* Cas9 used in this study carries at the C terminus an HA tag and two nuclear localization signal peptides that facilitate transport across the nuclear membrane. The protein was expressed with a N-terminal hexahistidine tag and maltose binding protein in *Escherichia coli* Rosetta 2 cells (EMD Millipore) from plasmid pMJ915. The His tag and maltose-binding protein were cleaved by TEV protease, and Cas9 was purified by the protocols described in Jinek et al. (1). Cas9 was stored in 20 mM Hepes at pH 7.5, 150 mM KCl, 10% glycerol, 1 mM TCEP at −80 °C.

In Vitro T7 Transcription of sgRNA with PAGE Purification. The DNA template encoding for a T7 promoter, a 20-nt target sequence, and the chimeric sgRNA scaffold was assembled from synthetic oligonucleotides by overlapping PCR. Briefly, for the CXCR4 sgRNA template, the PCR contains 20 nM premix of SLKS3 (5′-TAA TAC GAC TCA CTA TAG GAA GCG TGA TGA CAA AGA GGG TTT TAG AGC TAT GCT GGA AAC AGC ATA GCA AGT TAA AAT AAG G -3′) and SLKS1 (5′-GCA CCG ACT CGG TGC CAC TTT TTC AAG TTG ATA ACG GAC TAG CCT TAT TTT AAC TTG CTA TGC TGT TTC CAG C-3′), 1 μM premix of T25 (5′-TAA TAC GAC TCA CTA TAG-3′) and SLKS1 (5′-GCA CCG ACT CGG TGC CAC TTT TTC AAG-3′), and 200 μM dNTP and Phusion Polymerase (NEB) according to the manufacturer's protocol. The thermocycler setting consisted of 30 cycles of 95 °C for 10 s, 57 °C for 10 s, and 72 °C for 10 s The PCR product was extracted once with phenol:chloroform:isoamylalcohol and then once with chloroform before isopropanol precipitation overnight at −20 °C. The DNA pellet was washed three times with 70% ethanol, dried by vacuum, and dissolved in DEPC-treated water. The PD-1 sgRNA template was assembled from T25, SLKS1, SLKS2, and SLKS11 (5′-TAA TAC GAC TCA CTA TAG CGA CTG GCC AGG GCG CCT GTG TTT TAG AGC TAT GCT GGA AAC AGC ATA GCA AGT TAA AAT AAG G-3′) by the same procedure.

A 100-μL T7 in vitro transcription reaction consisted of 30 mM Tris·HCl (pH 8), 20 mM $MgCl_2$, 0.01% Triton X-100, 2 mM spermidine, 10 mM fresh DTT, 5 mM of each ribonucleotide triphosphate, 100 μg/mL T7 Pol, and 0.1 μM DNA template. The reaction was incubated at 37 °C for 4 h, and 5 units of RNase-free DNaseI (Promega) was added to digest the DNA template 37 °C for 1 h. The reaction was quenched with 2× STOP solution (95% deionized formamide, 0.05% bromophenol blue, and 20 mM EDTA) at 60 °C for 5 min. The RNA was purified by electrophoresis in 10% polyacrylamide gel containing 6 M urea. The RNA band was excised from the gel, ground up in a 50-mL tube, and eluted overnight in 25 mL of 300 mM sodium acetate (pH 5) overnight at 4 °C with gentle rocking. The solution was then centrifuged at 4,000 × *g* for 10 min, and the RNA supernatant was passed through a 0.45-μm filter. One equivalent of isopropanol was added to the filtered supernatant to precipitate the RNA overnight at −20 °C. The RNA pellet was collected by centrifugation, washed three times with 70% ethanol, and dried by vacuum. To refold the sgRNA, the RNA pellet was first dissolved in 20 mM Hepes (pH 7.5), 150 mM KCl, 10% glycerol, and 1 mM TCEP. The sgRNA was heated to 70 °C for 5 min and cooled to room temperature. $MgCl_2$ was added to a final concentration of 1 mM. The sgRNA was again heated to 50 °C for 5 min, cooled to room temperature, and kept on ice. The sgRNA concentration was determined by OD_{260nm} using Nanodrop and adjusted to 100 μM using 20 mM Hepes (pH 7.5), 150 mM KCl, 10% glycerol, 1 mM TCEP, and 1 mM $MgCl_2$. The sgRNA was stored at −80 °C.

In Vitro T7 Transcription of sgRNA with Phenol/Chloroform Extraction. DNA templates for in vitro T7 transcription were generated by annealing complementing single-stranded ultramers (Ultramer sequences: CXCR4_1: 5′-TAA TAC GAC TCA CTA TAG GAA GCG TGA TGA CAA AGA GGG TTT TAG AGC TAT GCT GGA AAC AGC ATA GCA AGT TAA AAT AA GGC TAG TCC GTT ATC AAC TTG AAA AAG TGG CAC CGA GTC GGT G-3′; CXCR4_2: 5′-CAC CGA CTC GGT GCC ACT TTT TCA AGT TGA TAA CGG ACT AGC CTT ATT TTA ACT TGC TAT GCT GTT TCC AGC ATA GCT CTA AAA CCC TCT TTG TCA TCA CGC TTC CTA TAG TGA GTC GTA TTA-3′; PD-1_1: 5′-TAA TAC GAC TCA CTA TAG CGA CTG GCC AGG GCG CCT GTG TTT TAG AGC TAT GCT GGA AAC AGC ATA GCA AGT TAA AAT AAG GCT AGT CCG TTA TCA ACT TGA AAA AGT GGC ACC GAG TCG GTG C-3′; PD-1_2: 5′-GCA CCG ACT CGG TGC CAC TTT TTC AAG TTG ATA ACG GAC TAG CCT TAT TTT AAC TTG CTA TGC TGT TTC CAG CAT AGC TCT AAA ACA CAG GCG CCC TGG CCA GTC GCT ATA GTG AGT CGT ATT A-3′). Ultramers were mixed in a 1:1 ratio in

nuclease-free duplex buffer (IDT) and heated up to 95 °C for 2 min followed by a 30-min incubation at room temperature.

A 100-μL T7 in vitro transcription reaction contained 1× Transcription Optimized buffer (Promega), 10 mM fresh DTT, 2 mM of each ribonucleotide triphosphate, 400 U T7 Pol (Promega), 0.5 U pyrophosphatase (Life Technologies), and 2 μg DNA template. The reaction was incubated for 4 h at 37 °C. Five units of RNase-free DNaseI (Promega) were added to digest the DNA template at 37 °C for 30 min. The reaction was stopped with 5 μL 0.5 M EDTA.

Given concern for the possibility of nucleic acid exchange between wells during PAGE purification, we tested phenol/chloroform-purified sgRNAs side by side with PAGE-purified sgRNAs as indicated in Fig. 4 and Fig. S1*A*. Phenol/chloroform extraction was performed after addition of 190 μL RNA-free H_2O. sgRNA was precipitated with 80 μL 3 M sodium acetate and 420 μL isoproponal and incubation at −20 °C for 4 h. The RNA pellet was washed twice with 70% EtOH and once with 100% EtOH. The vacuum-dried pellet was reconstituted, and the sgRNAs refolded as described in *In Vitro T7 Transcription of sgRNA with PAGE Purification.*

Cas9 RNP Assembly and Electroporation. Cas9 RNP was prepared immediately before experiments by incubating 20 μM Cas9 with 20 μM sgRNA at a 1:1 ratio in 20 μM Hepes (pH 7.5), 150 mM KCl, 1 mM $MgCl_2$, 10% glycerol, and 1 mM TCEP at 37 °C for 10 min to a final concentration of 10 μM.

T cells were electroporated with a Neon transfection kit and device (Invitrogen). A total of 2.5×10^5 T cells was washed three times with PBS before resuspension in 8 μL of buffer T (Neon kit, Invitrogen). Cas9 RNP (2 μL of 10 μM Cas9 CTRL without sgRNA or 1–2 μL Cas9:sgRNA RNP; final concentration: 0.9–1.8 μM) and HDR template (0–200 pmol as indicated) were added to the cell suspension to a final volume of 11 μL (adjusted with Cas9 storage buffer) and mixed. Ten microliters of the suspension was electroporated with a Neon electroporation device (Invitrogen; 1,600 V, 10 ms, three pulses). The HDR templates for CXCR4 and PD-1 are single-stranded oligonucleotides complementary (- strand) to the target sequence and contain a HindIII restriction sequence along with 90-nt homology arms. Upon successful HDR, the respective PAM sites are deleted, which should prevent recutting of the edited site by the Cas9 RNPs. The PD-1 HDR template additionally causes a frameshift and nonsense mutation as early as amino acid position 25 by replacing 12 nt with 11 nt (CXCR4 HDR template: 5′-GGG CAA TGG ATT GGT CAT CCT GGT CAT GGG TTA CCA GAA GAA ACT GAG AAG CAT GAC GGA CAA GTA CAG GCT GCA CCT GTC AGT GGC CGA AAG CTT GGA TCC CAT CAC GCT TCC CTT CTG GGC AGT TGA TGC CGT GGC AAA CTG GTA CTT TGG GAA CTT CCT ATG CAA GGC AGT CCA TGT CAT CTA CAC AGT-3′; PD-1 HDR template: 5′-AAC CTG ACC TGG GAC AGT TTC CCT TCC GCT CAC CTC CGC CTG AGC AGT GGA GAA GGC GGC ACT CTG GTG GGG CTG CTC CAG GCA TGC AGA TAA TGA AAG CTT CTG GCC AGT CGT CTG GGC GGT GCT ACA ACT GGG CTG GCG GCC AGG ATG GTT CTT AGG TAG GTG GGG TCG GCG GTC AGG TGT CCC AGA GC-3′). The CXCR HDR control donor is a sequence scrambled version on the original CXCR4 HDR template containing a HindIII restriction site (CXCR4 control HDR template: 5′-TTC AAA ACT AGC GTC AGG GGC TCG ATT TAC TCG GGA CTT GCT ACA ACA TCG CAG TCA CGC GCA CGA TCC TTC CAG GAT TGG AGG TGG ACT TAG ATA AAG CTT CCG TGT GCA CCG TAT AGA TTC GTT GAT GCA GGC TAT TCC CGT GAT CCC ACG CGG AGG TGA TGG AGC GTC AAG CAT AGC TAG CAC AGA TGA-3′).

Electroporated T cells were transferred to 500 μL of their respective culture medium in a αCD3/CD28-coated 48-well plate. Plates were coated with 10 μg/mL αCD3 (UCHT1; BD Pharmingen) and αCD28 (CD28.2; BD Pharmingen) in PBS for at least 2 h at 37 °C. Twenty-four hours after electroporation cells were resuspended and transferred to a noncoated well plate. Three to four days after electroporation, T cells were analyzed by FACS and T7 endonuclease I assay.

FACS Analysis of Edited T Cells. CXCR4 cell-surface staining was performed with αCXCR4-APC (12G5; BD Pharmingen) and αPD-1-PE (EH12.2H7; Biolegend) for 15 min on ice. Cells were kept at 4 °C throughout the staining procedure until cell sorting to minimize antibody-mediated internalization and degradation of the antibody. Cells were sorted using a FACS Aria Illu (Becton Dickinson).

PCR Amplification of Target Region. A total of 5×10^4 to 2×10^5 cells were resuspended in 100 μL of Quick Extraction solution (Epicenter) was added to lyse the cells and extract the genomic DNA. The cell lysate was incubated at 65 °C for 20 min and then at 95 °C for 20 min and stored at −20 °C. The concentration of genomic DNA was determined by NanoDrop (Thermo Scientific).

Genomic regions, containing the CXCR4 or PD-1 target sites, were PCR-amplified using the following primer sets: for CXCR4—forward 5′-AGA GGA GTT AGC CAA GAT GTG ACT TTG AAA CC-3′ and reverse 5′-GGA CAG GAT GAC AAT ACC AGG CAG GAT AAG GCC-3′ (938 bp); and for PD-1—forward 5′-GGG GCT CAT CCC ATC CTT AG-3′ and reverse 5′-GCC ACA GCA GTG AGC AGA GA-3′ (905 bp). Both primer sets were designed to avoid amplifying the HDR templates by annealing outside of the homology arms. The PCR contained 200 ng of genomic DNA and Kapa Hot start high-fidelity polymerase (Kapa Biosystems) in high GC buffer according to the manufacturer's protocol. The thermocycler setting consisted of one cycle of 95 °C for 5 min, 35 cycles of 98 °C for 20 s, 62 °C for *CXCR4* or 68 °C for *PD-1* for 15 s, and 72 °C for 1 min, and 1 cycle of 72 °C for 1 min. The PCR products were purified on 2% agarose gel containing SYBR Safe (Life Technologies). The PCR products were eluted from the agarose gel using QIAquick gel extraction kit (Qiagen). The concentration of PCR DNA was quantitated with a NanoDrop device (Thermo Scientific). A total of 200 ng of PCR DNA was used for T7 endonuclease I and HindIII analyses. For Fig. 1*E*, PCR product was cloned with TOPO Zero Blunt PCR Cloning Kit (Invitrogen) and submitted for Sanger sequencing.

Analysis of Editing Efficiency by T7 Endonuclease I Assay. Editing efficiency was estimated by T7 endonuclease I assay. T7 endonuclease I recognizes and cleaves mismatched heteroduplex DNA that arises from hybridization of wild-type and mutant DNA strands. The hybridization reaction contained 200 ng of PCR DNA in KAPA high GC buffer and 50 mM KCl and was performed on a thermocycler with the following setting: 95 °C, 10 min, 95–85 °C at −2 °C/s, 85 °C for 1 min, 85–75 °C at −2 °C/s, 75 °C for 1 min, 75–65 °C at −2 °C/s, 65 °C for 1 min, 65–55 °C at −2 °C/s, 55 °C for 1 min, 55–45 °C at −2 °C/s, 45 °C for 1 min, 45–35 °C at −2 °C/s, 35 °C for 1 min, 35–25 °C at −2 °C/s, 25 °C for 1 min, and hold at 4 °C. Buffer 2 and 5 units of T7 endonuclease I (NEB) were added to digest the reannealed DNA. After 1 h of incubation at 37 °C, the reaction was quenched with 6× blue gel loading dye (Thermo Scientific) at 70 °C for 10 min. The product was resolved on 2% agarose gel containing SYBR gold (Life Technologies). The DNA band intensity was quantitated using Image Lab. The percentage of editing was calculated using the following equation $[1 - (1 - (b + c/a + b + c))^{1/2}] \times 100$, where a is the band intensity of DNA substrate and b and c are the cleavage products. For the quantification of the *PD-1* T7E1 assay (Fig. 4*D*), the intensity of the DNA substrate was calculated as the sum of the two large bands seen under all conditions. Calculation of the percentage of total edit based on T7E1 assays allows only an estimate of cleavage efficiency.

Analysis of HDR by HindIII Restriction Digestion. HDR templates were designed to introduce a HindIII restriction site into the targeted

gene locus. To test for successful introduction of the HindIII site into the CXCR4 locus, the 938-bp region was PCR-amplified using the primers 5′-AGA GGA GTT AGC CAA GAT GTG ACT TTG AAA CC-3′ and 5′-GGA CAG GAT GAC AAT ACC AGG CAG GAT AAG GCC-3′. For the *PD-1* locus, a 905-bp region was amplified using the primers 5′-GGG GCT CAT CCC ATC CTT AG-3′ and 5′-GCC ACA GCA GTG AGC AGA GA-3′. The reaction consisted of 200 ng of PCR DNA and 10 units of HindIII High Fidelity in CutSmart Buffer (NEB). After 2 h of incubation at 37 °C, the reaction was quenched with 1 vol of gel loading dye at 70 °C for 10 min. The product was resolved on 2% agarose gel containing SYBR gold (Life Technologies). The band intensity was quantitated using Image Lab. The percentage of HDR was calculated using the following equation: $(b + c/a + b + c) \times 100$, where a is the band intensity of DNA substrate and b and c are the cleavage products.

Deep-Sequencing Analysis of On-Target and Off-Target Sites. The genomic region flanking the Cas9 target site for the CXCR4 on-target and two off-target genes was amplified by the two-step PCR method using the following primers: CXCR4 on-target (5′-ACA CTC TTT CCC TAC ACG ACG CTC TTC CGA TCT NNN NNC TTC CTG CCC ACC ATC TAC TCC ATC ATC TTC TTA ACT G-3′ and 5′-GTG ACT GGA GTT CAG ACG TGT GCT CTT CCG ATC TNN NNN CAG GTA GCG GTC CAG ACT GAT GAA GGC CAG GAT GAG GAC-3′); off-target #1 [*POU domain*, *class 2*, *transcription factor 1 isoform 1* (*POU2F1*)] locus; 5′-ACA CTC TTT CCC TAC ACG ACG CTC TTC CGA TCT NNN NNG CTA TAA TAG TAC AAG TAT ATG TTA AAT AAG AGT CAT AGC ATG-3′ and 5′-GTG ACT GGA GTT CAG ACG TGT GCT CTT CCG ATC TNN NNN CTG GCT TTA TAT ATA TAC ATA GAT AGA CGA TAT AGA TAG C-3′); and off-target #2 [*glutamate receptor 1 isoform 1 precursor* (*GRIA1*)] locus; 5′-ACA CTC TTT CCC TAC ACG ACG CTC TTC CGA TCT NNN NNC CTG GTC CCA GCC CAG CCC CAG CTA TTC AGC ATC C-3′ and 5′-GTG ACT GGA GTT CAG ACG TGT GCT CTT CCG ATC TNN NNN ACT CTG CAC TGG TAT ATC AAT ACA CTT GTT TTT CTC ATC CC-3′). First, 100–150 ng of the genomic DNA from the edited and control samples was PCR-amplified using Kapa Hot start high-fidelity polymerase (Kapa Biosystems) according to the manufacturer's protocol. The thermocycler setting consisted of one cycle of 95 °C for 5 min and 15–20 cycles of 98 °C for 20 s, 63 °C for 15 s, 72 °C for 15 s, and one cycle of 72 °C for 1 min. The resulting amplicons were resolved on 2% agarose gel, stained with SYBR Gold, and gel-extracted using Qiagen gel extraction kit.

Illumina TruSeq Universal adapter (5′-AAT GAT ACG GCG ACC ACC GAG ATC TAC ACT CTT TCC CTA CAC GAC GCT CTT CCG ATC T-3′) and modified Illumina RNA PCR barcode primer (5′-CAA GCA GAA GAC GGC ATA CGA GAT-Index- GTG ACT GGA GTT CAG ACG TGT GCT CTT CCG ATC T-3′) were attached to the amplicon in the second PCR step using Kapa Hot start high-fidelity polymerase (Kapa Biosystems). The thermocycler setting consisted of one cycle of 98 °C for 30 s, 8–10 cycles of 98 °C for 20 s, 65 °C for 15 s, 72 °C for 15 s, and one cycle of 72 °C for 5 min. The resulting amplicons were resolved on 2% agarose gel, stained with SYBR Gold, and gel-extracted using a Qiagen gel extraction kit. Barcoded and purified DNA samples were quantified by Qubit 2.0 Fluorometer (Life Technologies), size-analyzed by BioAnalyzer (Agilent), quantified by qPCR, and pooled in an equimolar ratio. Sequencing libraries were sequenced with the Illumina HiSEq. 2500.

Analysis of Deep-Sequencing Data. Sequencing reads that contained the unique 12 nt resulting from the HDR template were extracted and analyzed separately from those that did not contain HDR template-derived sequence. All reads that did not contain the replaced 12 nt were aligned to the reference hg19 genome, and all of the reads that contained the replaced 12 nt were aligned to a modified hg19 genome with the expected substitutions using BWA. The samtools mpileup utility was then used to quantify the total number of reads that mapped to each position of the *CXCR4* gene, and a custom script examining the CIGAR string was used to estimate the number and locations of insertions and deletions for each read. Insertion efficiency was estimated for the experiment with CXCR4 RNP (without HDR template) as the following: (number of reads with insertions ±100 bp from cut site)/(total number of reads ± from cut site). For deletion efficiency the experiment with CXCR4 RNP (without HDR template) was estimated as the following: (number of reads with deletions ±100 bp from cut site)/(total number of reads ± from cut site). For experiments with CXCR4 RNP + HDR template, insertion and deletion efficiencies were calculated based only on reads that that did not contain the 12-nt replacement derived from HDR (these are the fractions shown in Fig. 3*B*). Total editing efficiency was estimated as (number of reads with indels ±100 bp from cut site)/(total number of reads ± from cut site). In Dataset S1, "%Indels in Total Reads" refers to total editing efficiency and includes reads with HDR template sequence incorporated except in rows where these reads have been removed. HDR efficiency was estimated as the following: (number of reads containing HindIII site ± 100 bp from cut site)/(total number of reads ± 100 bp from cut site). Distribution of insertion and deletion sizes were estimated for a region ± 20 bp from the cut site.

1. Jinek M, et al. (2012) A programmable dual-RNA-guided DNA endonuclease in adaptive bacterial immunity. *Science* 337(6096):816–821.

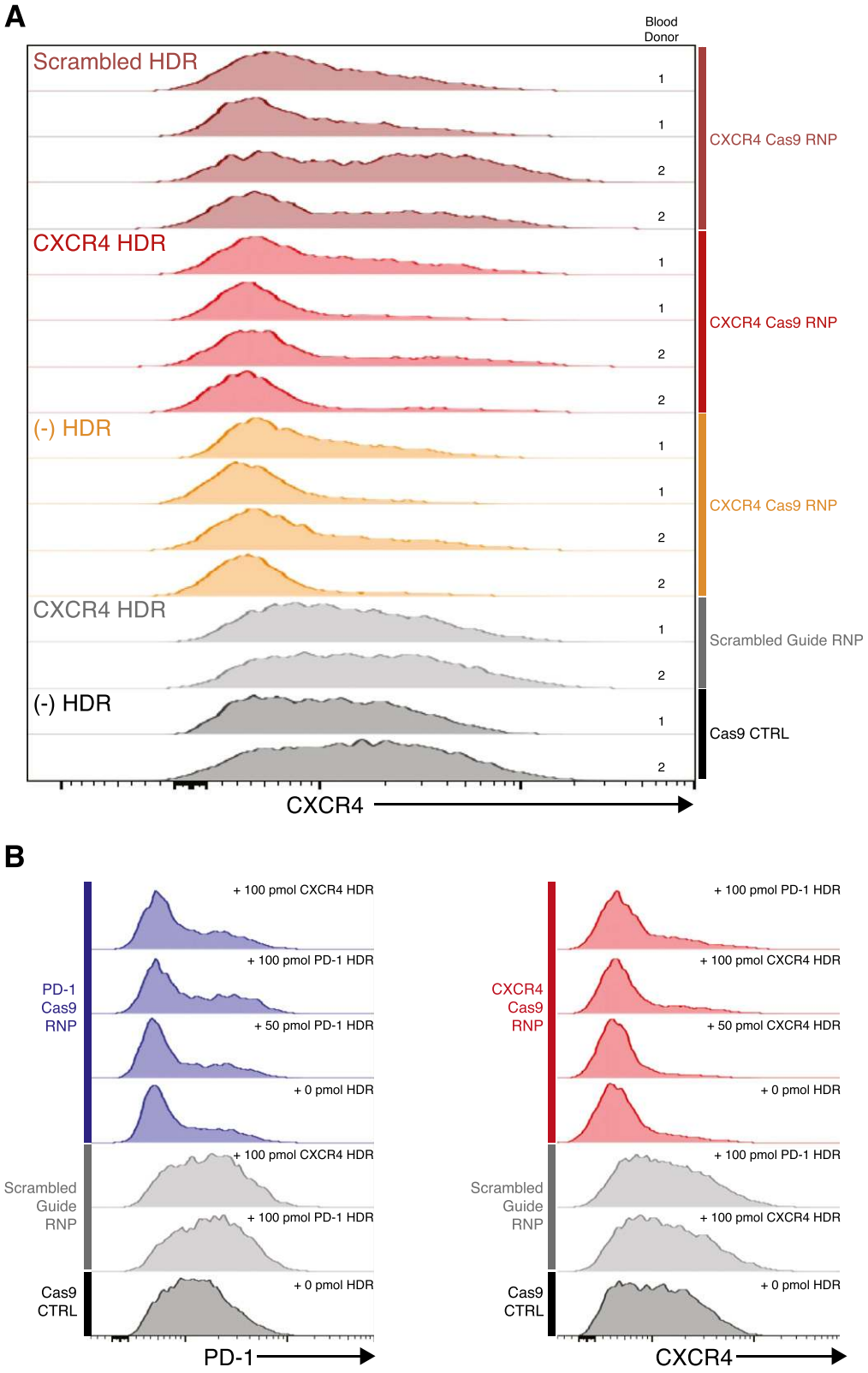

Fig. S1. Effects of "on-target" and control HDR templates on PD-1 and CXCR4 surface expression levels. (*A*) The effects on CXCR4 expression were tested for two different HDR templates with the same nucleotide composition. In cells that were treated with CXCR4 Cas9 RNP, CXCR4 HDR template (dark red) was compared with a control HDR template consisting of the same nucleotides as the original CXCR4 HDR in randomized order including a HindIII restriction site (light red) and with no HDR template treatment (orange). Further controls are Cas9 CTRL (Cas9 without sgRNA; dark gray) and scrambled guide Cas9 RNP (no predicted cut within the human genome) with 100 pmol CXCR4 HDR template (light gray). The histograms show the results of four experiments with two differently in vitro-transcribed CXCR4 sgRNAs (two different purification strategies; *Materials and Methods*) tested in two different blood donors. As in Fig. 4, for each blood donor, experiments done with phenol/chloroform-extracted sgRNAs are shown on *Top* and experiments with PAGE-purified sgRNAs are shown

Legend continued on following page

at the *Bottom*; scrambled guides were prepared for both experiments with phenol/chloroform extraction. (*B*) PD-1 (blue, *Left*) and CXCR4 (red, *Right*) surface expression levels after editing with the respective Cas9 RNPs and on- or off-target HDR templates. Targeted cells were compared with cells treated with Cas9 CTRL (dark gray) or scrambled guide Cas9 RNP (light gray).

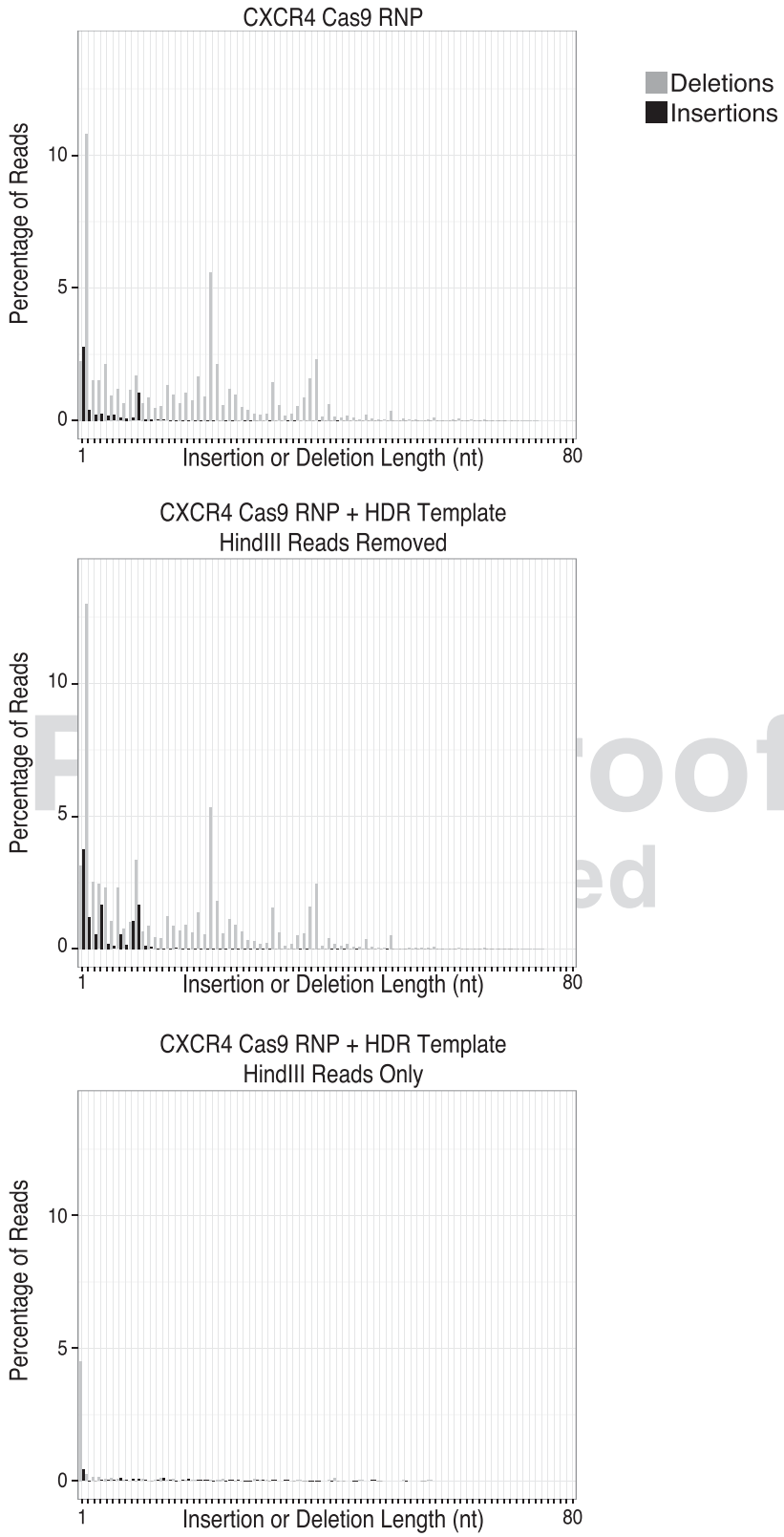

Fig. S2. Distribution of insertion and deletion lengths near expected CXCR4 cut site. Histograms show the percentage of reads that contain varying sizes of deletions (gray bars) and insertions (black bars) within ±20 nt of the predicted cut site. (*Top*) Insertions and deletions for CXCR4 RNP-treated cells. (*Middle*) Insertions and deletions in reads without HDR template-derived sequence incorporated in the cells treated with CXCR4 RNP and CXCR4 HDR template. (*Bottom*) Insertions and deletions in reads that did incorporate in the HDR template-derived sequence.

Dataset S1. Summary of editing frequencies based on deep sequencing

Dataset S1

Indicated are the numbers of reads (and percentages of total reads) with insertions, deletions, both insertions and deletions, or any indels in cells treated with Cas9, CXCR4 Cas9 RNP, and CXCR4 Cas9 RNP + HDR template (based on deep-sequencing results analyzed in Fig. 3). Here, "%Indels in Total Reads" refers to total editing efficiency and includes reads with HDR template sequence incorporated except in rows where these reads have been removed. Total number of reads with indels was calculated as the following: (no. of reads with insertions) + (no. of reads with deletions) – (no. of reads with insertions and deletions).

AUTHOR QUERIES

AUTHOR PLEASE ANSWER ALL QUERIES

Q: 1_In sentence beginning "The DNA pellet was washed..." please replace DEPC with its definition.

Q: 2_Please clarify "(- strand)" in sentence beginning "The HDR templates for..."

Q: 3_In sentence beginning "The hybridization reaction contained...." is "°C/s" as intended without number of seconds indicated here and below?

Q: 4_In sentence beginning "All reads that did not contain...." please replace "BWA" with its definition.